*De Waele, B., Johnson, S. P., Nkemba, S., and Tembo, F. 2005. High-temperature, low-pressure tectono-thermal evolution of the Irumide Belt, central Southern Africa: lithosphere delamination during arc-accretion. Frontier Research on Earth Evolution Report 2002-2004, V2. 9p.

High-temperature, low-pressure tectono-thermal evolution of the Irumide Belt, central, Southern Africa: Lithosphere delamination during arc-accretion.

B. De Waele[1], S. P. Johnson[2], S. Nkemba[3], and F. Tembo[3]

1: Tectonics Special Research Centre, School of Earth and Geographical Sciences, The University of Western Australia.
2: Program for Palaeoenvironment, Institute for Research in Earth Evolution.
3: School of Mines, Geology Department, University of Zambia.

1. Introduction

[1] The Irumide belt forms a narrow, northeast oriented region of deformed granitic basement, overlain by a supracrustal sequence and intruded by widespread granitoids, stretching from central Zambia to the Zambia-Tanzania border and into northern Malawi (Fig. 1). To the south and southeast, the Permo-Triassic Karoo grabens subdivide the Irumide Belt into two parts; the Irumide Belt (*s.s.)* and the Bangweulu Block to the north, and the Southern Irumide Belt to the southeast *[Johnson et al., in press*] (Fig. 1). The Irumide Belt (*s.s.)* comprises a basement of granitoid gneisses, aged between 2.05 and 1.93 Ga [*Rainaud et al.*, 2003; 2004b; *De Waele et al.*, 2004a], unconformably, and in places structurally, overlain by a metasedimentary succession, regionally defined as the Muva Supergroup [*Daly and Unrug*, 1982]. U-Pb zircon crystallisation ages (measured by SHRIMP) of interstratified rhyolitic tuffs within the supergroup indicate deposition between 1.88 and 1.85 Ga. This basement and supracrustals were intruded, first by a minor magmatic suite between 1.65 and 1.55 Ga, and later by voluminous K-feldspar-phyric granitoids between 1.05 and 0.95 Ga [*De Waele* et al., 2003]. These latest Mesoproterozoic granitoids were intruded in a similar time frame as collisional events in other cratons that are associated with the amalgamation of the Rodinia supercontinent, and have been used to uncritically demonstrate that that the Congo Craton was part of the supercontinent.

[2] In this paper we present new electron and ion microprobe data, to constrain both the pressure-temperature conditions and style of metamorphism and the timing of growth of metamorphic zircon overgrowths in the Irumide Belt (*s.s.*).

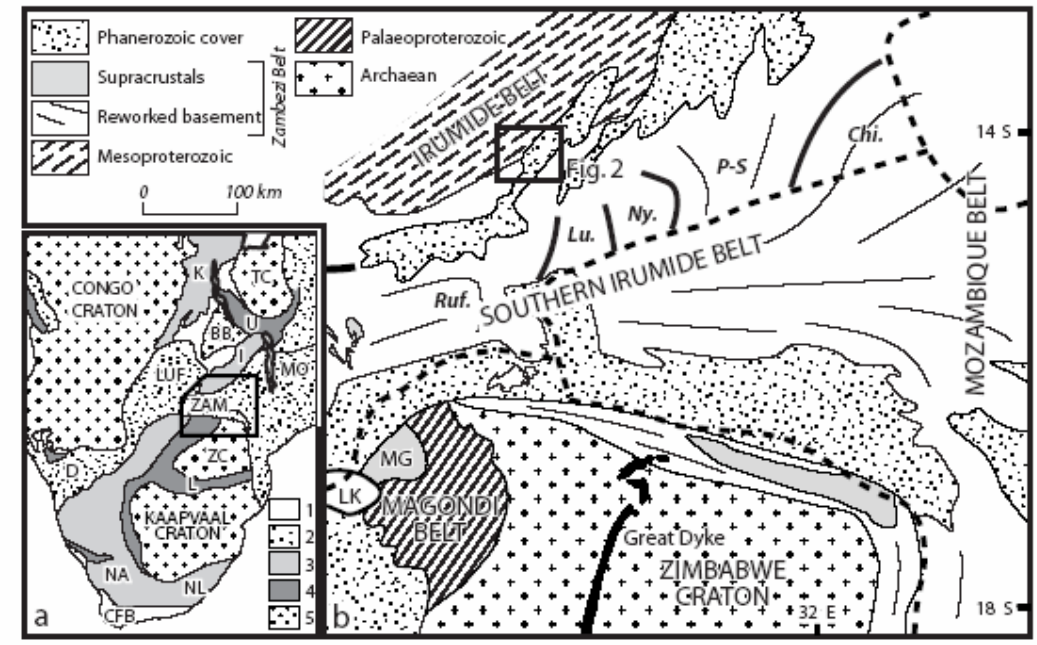

Figure 1: a) Tectonic map of Africa after Hanson, 2003. Box indicates location of main figure. Key: 1–Post Pan African Basins; 2–Pan African belts; 3–Mesoproterozoic Belts; 4–Palaeoproterozoic belts; 5–Archaean cratons. b) Simplified geological map of central, southern Africa. Box locates the Serenje area depicted in Figure 2. Abbreviations the same as Figure 1 except: CFB–Cape Fold Belt; Chi.–Chipata Terrane; CI–Chewore Inliers; CR–Chowe River area; D–Damara Belt; I–Irumide Belt; K–Kibaran Belt; L–Limpopo Belt; LK–Lake Kariba; Lu. Luangwa Terrane; LUF–Lufilian Belt; MG–Makuti Group; MO–Mozambique Belt; NA–Namaqua Belt; NL–Natal Belt; Ny. Nyimba Terrane; P-S–Petauke-Sinda Terrane; TC–Tanzanian Craton; U–Ubendian Belt; ZAM–Zambezi Belt; ZC–Zimbabwe Craton.

2. Previous Metamorphic Studies

[3] The general distribution of metamorphic facies in Zambia was described by *Ramsay and Ridgway* [1977] and later discussed by *Ramsay and Ridgeway* [1977] and *Vrána* [1979], that resulted in the publication of a metamorphic map of Zambia [*Ridgway and Ramsay*, 1986]. According to that map, the Irumide Belt lies entirely in the Luangwa-Kariba metamorphic zone and is characterised by a range of metamorphic facies, from sub-greenschist to greenschist facies in the northwest, up to the amphibolite and localised granulite facies to the southeast. The change in metamorphic assemblages is best seen in the Serenje area (Figs. 1 and 2) where metapelites consistently record the metamorphic assemblages muscovite + chlorite + quartz + albite + talc ± epidote or muscovite + biotite + albite + quartz in the northeastern part of the area, increasing towards the southwest, where staurolite + muscovite + garnet and cordierite + andalusite appear, with in the extreme southwestern corner of the map sheet, sillimanite + garnet + amphibole and sillimanite + garnet + biotite recorded in migmatites and metapelites [*Mapani*, 1992; 1999; *Mapani and Moore*, 1995]. The latter mineral assemblage being diagnostic of the granulite facies. In other places kyanite is present but appears to be locally restricted rather than of a regional nature. In the Southern Irumide Belt (Fig. 1), the presence of sillimanite + garnet assemblages, and local occurrence of kyanite appear to confirm regional amphibolite facies conditions similar to those described in the Irumide Belt (*s.s.*). In addition, *Barr and Drysdall* [1972] and *Phillips* [1965] report diopside + clinozoisite assemblages in marbles and sillimanite + garnet in adjacent pelitic units between Mvuvye and Petauke, also suggesting amphibolite grades, while local hypersthene + antiperthite granulites indicate granulite grade metamorphism [*Phillips*, 1964; *Agar and Ray*, 1983]. Because of the lack of age data, and the clear evidence of multiple deformations in the Southern Irumide belt, some attributed to Irumide, some to Zambezi tectonism [*Johns et al*., 1989], it is unclear whether these assemblages record metamorphic conditions during Irumide orogenesis or during the successive Zambezi Orogen. The only age data for metamorphism in the region are provided by *Cox et al*., [2002] who report a Laser Ablation Inductively Coupled Plasma Mass Spectrometer (LA-ICP-MS) age of 1043 ± 19 Ma for low Th/U rim overgrowths on zircon from a diorite near Luangwa Bridge. In the same region, *John et al*. [1999] reported peak metamorphic conditions of 650°C at 6 kbar for sillimanite + garnet + muscovite + biotite schists, which can tentatively be ascribed to the metamorphic event dated in the rims. Further east, near the town of Chipata (Fig 1), *Schenk and Appel* [2001, 2002] reported a similar age of 1046 ± 3 Ma for a monazite, interpreted to have crystallised during peak metamorphism, for which 875-900°C at 6kbar were calculated based on thermo-barometric calculations on the garnet + sillimanite + cordierite + spinel + quartz gneiss from which is was extracted. This seems to indicate ultra-high temperature metamorphic conditions at ca. 1.05 Ga, which *Schenk and Appel* [2001; 2002] attributed to the intrusion and loading of granitic magmas in the region.

3. Petrology and Thermobarometry

3.1. Field relationships

[4] The samples used for thermobarometric analyses were collected from the southwestern portion of the Serenje map sheet, where a wide swath of migmatites and high-grade garnet-sillimanite metapelites were reported by *Mapani and Moore* [1995] (Fig. 2). The migmatites were sampled along the Lukusashi and Fukwe rivers (Fig. 2) and all contain quartz + plagioclase + microcline + biotite + garnet + muscovite, while samples KS23, KS27c, SER7 and SER15 additionally contain abundant sillimanite. The melanosomes consist of biotite + quartz + plagioclase + garnet ± sillimanite with accessory apatite, whilst the leucosomes consist of quartz + microcline + plagioclase, accessory garnet ± sillimanite and occasionally beryl and/or tourmaline. Where the rocks are strongly segregated, banding is defined by nebulitic and stromatic structures, and cross-cut by ptygmatically folded quartz-feldspar veins. All lithologies carry a strong, northeast-directed crenulation lineation that is defined by aligned micas, and where present, sillimanite needles and elongated sillimanite-biotite clots. The Fukwe Gneiss (samples KS27 and SER7) contains garnet- and sillimanite-rich melanosomes in which garnet porphyroblasts demonstrate sinistral shear rotation during the fabric-forming event. Where stromatic and nebulitic patterns are less strongly developed, the rocks are tightly and irregularly folded with upright to inclined northeast-southwest oriented axial planes and shallow (10-20°), northeast-plunging fold hinges.

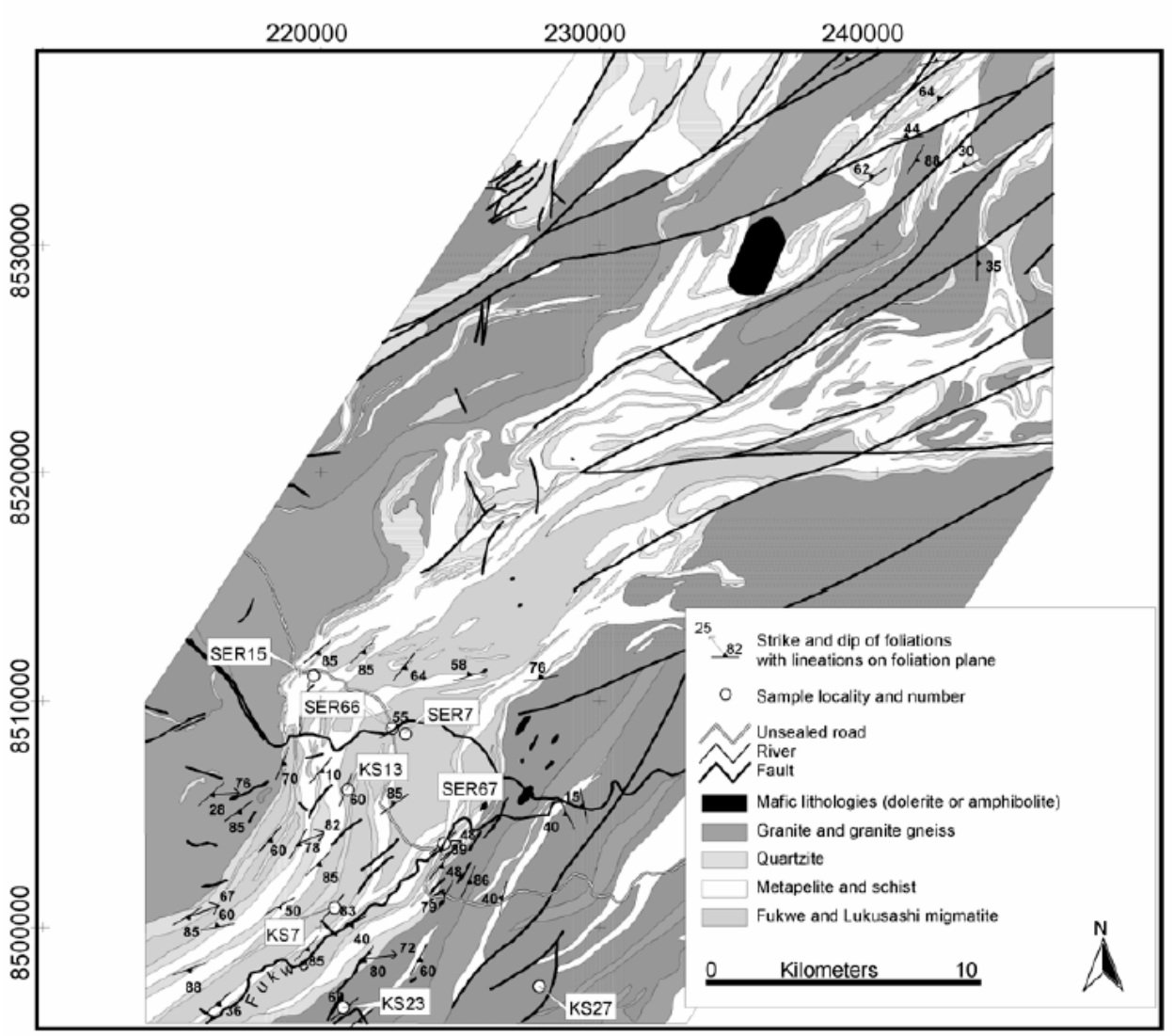

Figure 2: Geological map of the Serenje Area after *Mapani and Moore*, [1995], showing PT and Geochronological sampling points.

3.2 *PT* Estimations

[5] Mineral compositions were analysed by electron microprobe analyser (EPMA) at the University of Western Australia. Operating conditions were 15keV acceleration voltage with a 5nA beam current and a working distance of 36 mm. All samples contain almandine-rich garnet that display relatively homogeneous compositions from core to rim (Fig. 3a-c) indicative of only a minor pressure increase during metamorphism. Plagioclase ranges from ~ 60–70% albite and biotite has decreasing XMg compositions of ~65% in the core to 35% in the rims. In sample SER 7 inclusions of both biotite and plagioclase within garnet allowed the calculation of the prograde PTt path. Most rim compositions appear to have undergone variable amounts of post-peak metamorphic re-equilibration and thus define a range of calculated PT's that represent conditions during retrograde metamorphism. Using the garnet-biotite geothermometer of *Ferry and Spear with Bermann* [1990] and the garnet-plagioclase-biotite-quartz geobarometer of *Hoish* [1990], mineral core PT's (i.e., conditions during the early stages of metamorphism) are estimated at 560°C and 2 kbar, whilst peak metamorphic conditions, obtained from the highest PT estimations from the rim assemblages, were 700°C at 5 kbar (Fig. 3d). Thus, metamorphism followed a low-pressure, moderate- to high-temperature path consistent with the regional abundance of sillimanite and the melting of pelitic and granitic lithologies (i.e., migmatization).

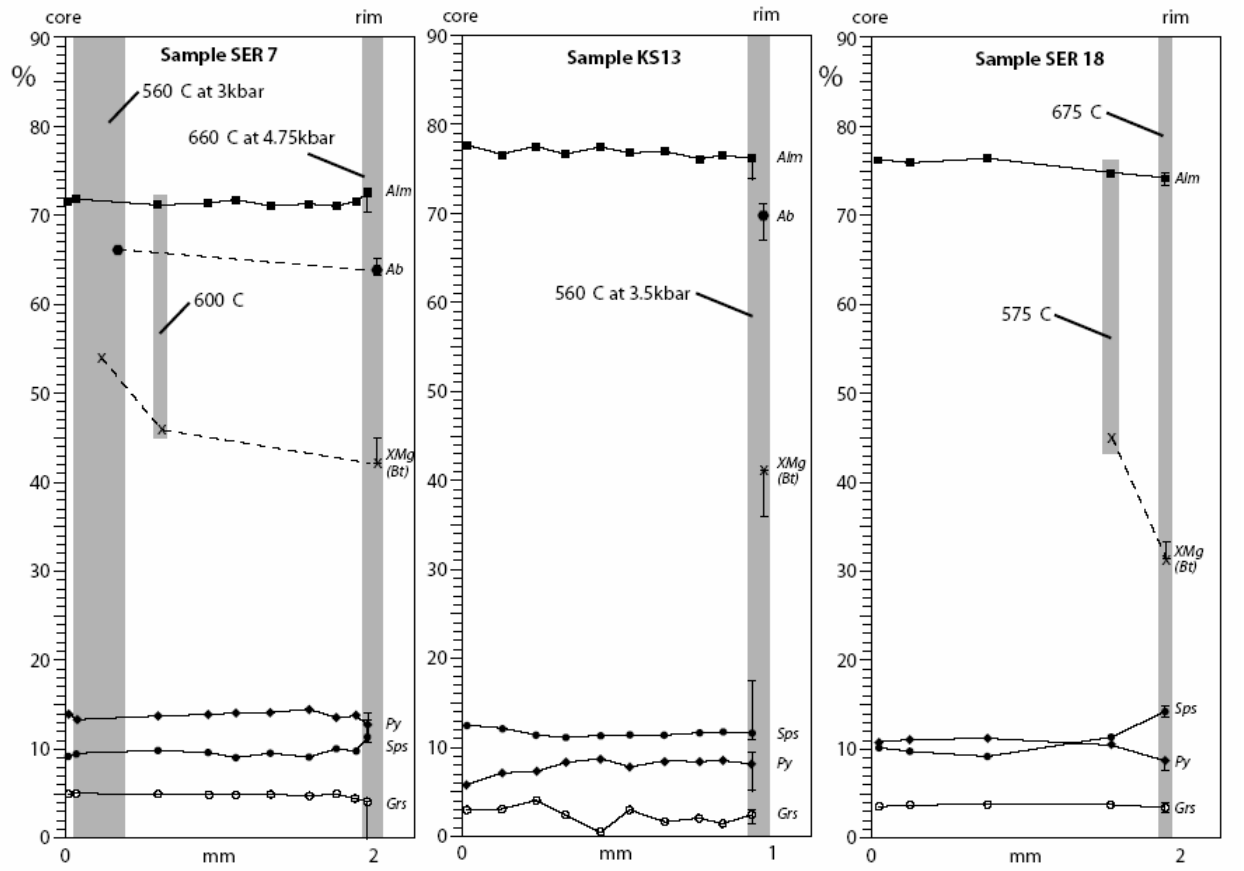

Figure 3: a-c) Geochemical profiles of garnet porphyroblasts from their core to rim, including the composition of biotite and plagioclase inclusions and rim compositions. Abbreviations: Ab–albite; Alm–almandine; Bt–biotite; Grs–grossular; Sps–spessartine.

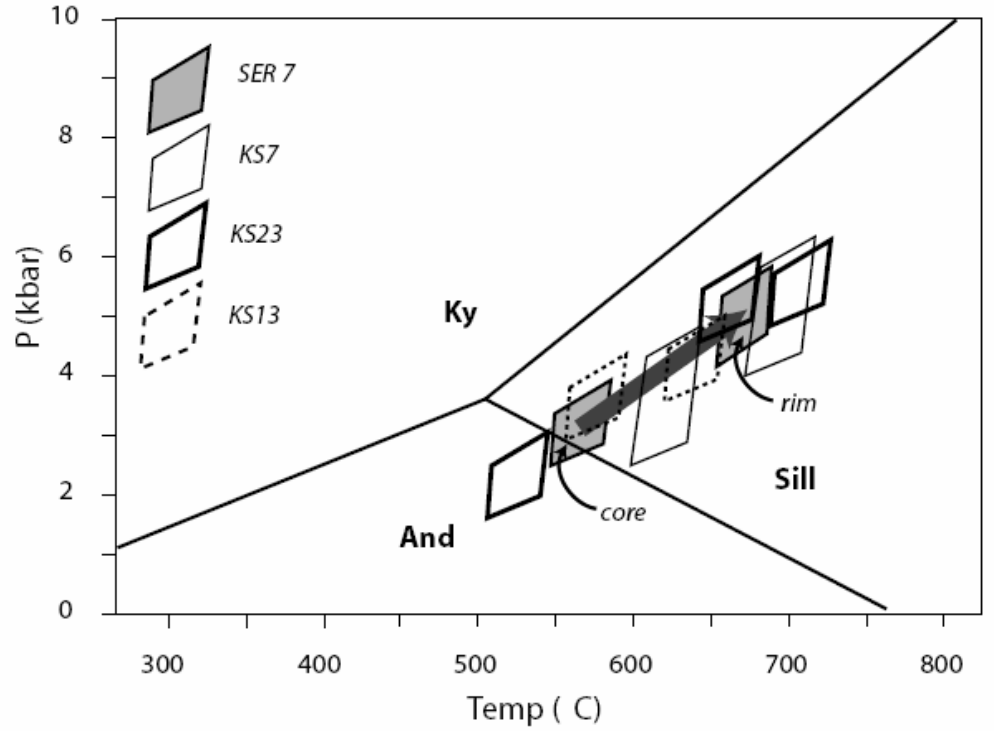

Figure 3: d) Pressure-Temperature diagram summarising the PTt evolution of samples. Abbreviations: And–andalusite; Ky–kyanite; Sill–sillimanite.

4. Zircon U-Pb SHRIMP Geochronology

4.1. The Lukusashi Migmatite

[6] A sample of the Lukusashi Migmatite (SER66) was collected at the crossing of the Chisomo road over the Lukusashi River (Fig. 2). The extracted zircons are complex in structure, and contain a core, often broken, but sometimes euhedrally preserved, surrounded by low-response (in CL) overgrowths (Fig 4a). The U-Pb-Th isotope ratios were analysed on the Perth Consortium **S**ensitive **H**igh-**R**esolution **I**on **M**icro**P**robe (SHRIMP II) at the Curtin University of Technology, Western Australia following the operating procedures of *Nelson* [1997]. Taken together, Th/U ratios range from 0.07 to 0.84 for the cores, and are very low (0.03 or smaller) for the rims. The consistent extremely low Th/U ratios, coupled with the absence of concentric zoning, strongly support the interpretation that the extensive high-uranium rims have formed during high-grade metamorphism [e.g. *Rubatto and Gebauer*, 2000]. A total of six cores were analysed, five of which are within 5% of concordia and form a coherent age group with an upper intercept of 2053 ± 11 Ma and lower intercept at –154 ± 320 Ma (MSWD=0.90) (Fig. 4e). A weighted mean $^{207}Pb/^{206}Pb$ age of 2050 ± 8 Ma (MSWD=0.89) can be calculated on all six data points and this is interpreted as the crystallisation age of the granitic protolith to the Lukusashi Migmatite.

[7] Ten analyses were made of the wide-rim zircon overgrowths. U is high, between 1486 and 3138 ppm, while Th is low, ranging from 12 to 37 ppm. The data plot within 5% of concordia and have a weighted mean $^{207}Pb/^{206}Pb$ age of 1018 ± 5 Ma (MSWD=0.69) (Fig. 4c) and is taken as the best estimate for the timing for the growth of the metamorphic rims.

4.2. The Fukwe Migmatite

[8] Sample SER67 was collected at the crossing of the Chisomo road with the Fukwe River (Fig. 2). Again the extracted zircons were equally complex, displaying inherited cores, and high-U overgrowths (Fig. 4b). Eight analyses were conducted on the cores, six of which yield an upper intercept age of 2023 ± 11 Ma with a lower intercept at 0 ± 140 Ma (MSWD=0.86) (Fig. 4e). The same points yielded a weighted mean $^{207}Pb/^{206}Pb$ age of 2023 ± 9 Ma (MSWD=0.69), and again is interpreted as the crystalisation age of the protolith granitoid.

[9] Twelve of the high-U rims were analysed. U content is high, between 913 and 1632 ppm, and Th very low, between 7 and 48 ppm, yielding low Th/U ratios less than 0.03 typical for metamorphic rims. One data point plots about 10% away from the concordia, and defines a $^{207}Pb/^{206}Pb$ age of 554 ± 20 Ma (SER67-3r). The analysis exhibits an extremely low Th/U value and represents the first reliable constraint on Pan African metamorphic overprinting in the region. Eight rims plot in a cluster close to concordia (Fig. 4d) and yield a weighted mean $^{207}Pb/^{206}Pb$ age of 1021 ± 16 Ma (MSWD=1.2), which is the best estimate for high-grade metamorphism and migmatisation of this rock.

4.3. The Chilubanama Granite

[10] One sample was collected for geochronological work from the Chilubanama Granite (Chinsali map sheet). Zircons from this sample (MTG4) are equant to elongate, euhedral and concentrically zoned. CL imaging reveals rounded and irregular, zoned and unzoned cores in about 75% of the grains, surrounded by low CL response rims. U and Th range from 124 to 1201 ppm and 9 to 820 ppm respectively, with Th/U ranging from 0.02 to 1.34. Th/U for analyses MTG4-4r, 8r, 9r and 10r are below 0.1, suggesting these zircon rims developed during metamorphism. The equally low Th/U ratio of core MTG4-10c may reflect solid-state recrystallisation of this zircon during the same metamorphic event. The oldest cores analysed (MTG4-7c, MTG4-4c and MTG4-1c) yielded $^{207}Pb/^{206}Pb$ ages of 2045 ± 11 Ma (106% concordant), 2017 ± 17 Ma (97% concordant) and 2010 ± 8 Ma (98% concordant; Fig. 4f) and the calculated ages are interpreted as approximating the crystallisation of these zircons in their protolith. Another core (MTG4-8c) yielded a $^{207}Pb/^{206}Pb$ age of 1425 ± 47 Ma (98 % concordant). The Chilubanama Granite thus appears to have sampled sources with these ages. The remaining nine data points, which comprise four cores (MTG4-5c, 6c, 9c and 10c) and five rims (MTG4-1r, 4r, 8r, 9r and 10r) are over 90% concordant and define a coherent age group with weighted mean $^{207}Pb/^{206}Pb$ age of 1019 ± 13 Ma (MSWD=1.6) (Fig. 4f). It appears that the low Th/U rims developed very soon after crystallisation of the magmatic zircon and that igneous crystallisation and metamorphism are statistically indistinguishable. The granite thus appears to have been emplaced during a metamorphic event dated at 1019 ± 13 Ma.

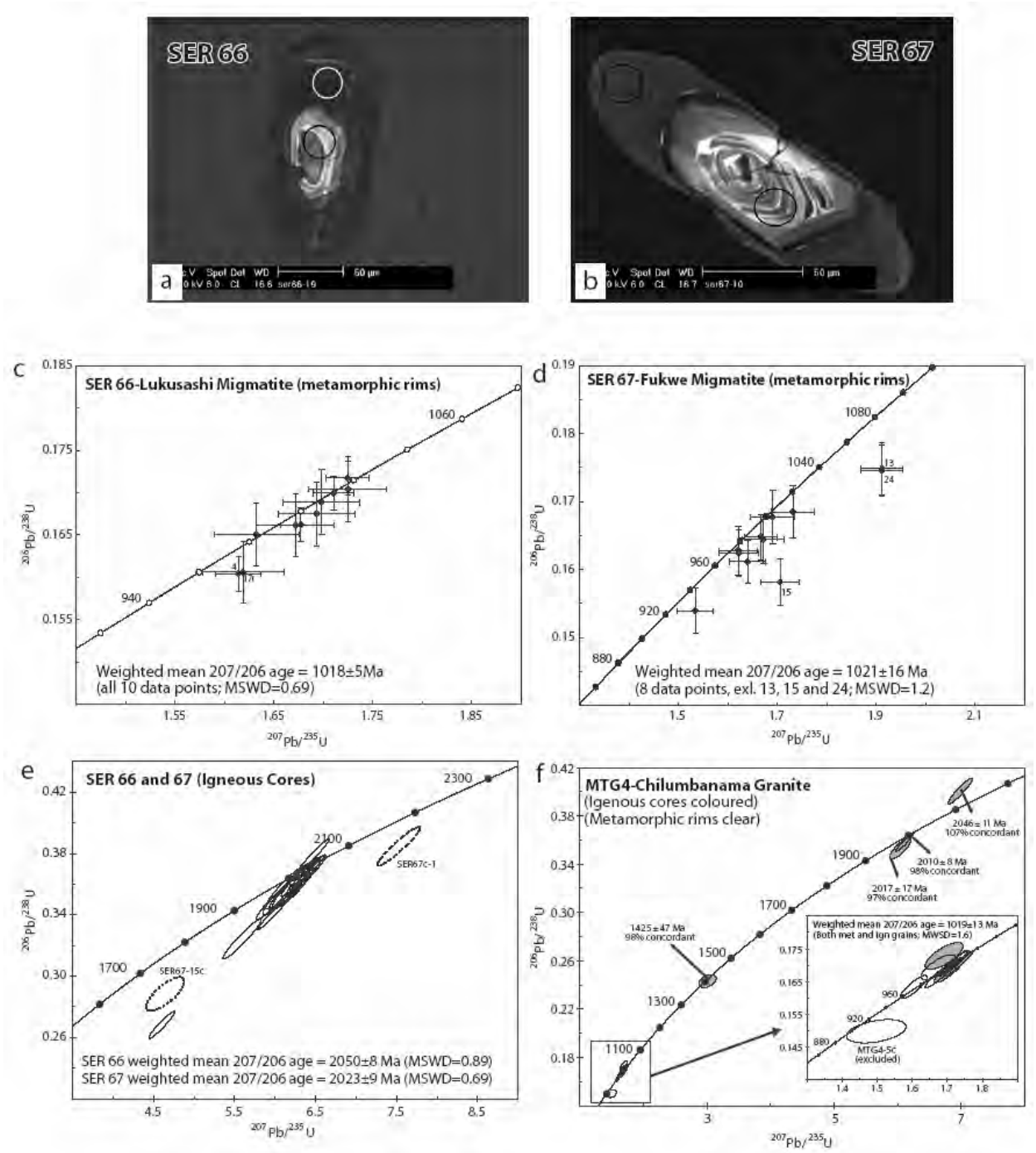

Figure 4: a-b) Cathodoluminescence images of zircons from SER 66 and SER 77, showing igneous, oscillatory-zoned cores surrounded by large, metamorphic overgrowths. c-f) U-Pb weheterill plots of the SHRIMP data.

4.4. Summary of U-Pb data

[11] The protolith age of both the Lukusashi as Fukwe migmatites is between 2050 and 2020 Ma and were subsequently metamorphosed at ca. 1021–1019 Ma, accompanied by the intrusion of the Chilubanama Granite.

5. Discussion

[12] The *PT* and geochronological data presented here indicate that the Irumide Belt underwent limited contractional deformation at ca. 1020 Ma under high-temperature, low-pressure conditions. This was the result of emplacement of voluminous K-feldspar-phyric granitoids between 1050–950 Ma [*De Waele et al*., 2004a, b]. At this time, the basement into which these granitoids were emplaced would have been located at the edge of the Congo Craton margin. Continental margins that are dominated by voluminous magmatism are commonly associated with subduction of oceanic crust beneath them, i.e., they are continental-margin-arcs like the present-day Andes. Magmatism within these arcs are predominantly of a juvenile character; however, all of the Irumide Belt granitoids have S-type characteristics, displaying very negative $\varepsilon_{Nd}(t)$ whole rock [*De Waele et al*., 2004a] and $\varepsilon_{Hf}(t)$ zircon [*Johnson unpublished data*] values, indicating that they formed by the direct melting and recycling of the basement. This data therefore negates any involvement of subduction of oceanic crust under the Congo Craton at this time.

[13] The Southern Irumide Belt is interpreted to represent a series of exotic terranes of supra-subduction origin, and associated sedimentary deposits, that accreted to the southern margin of the Congo Craton during the Late Mesoproterozoic [*Johnson et al., in press*]. Supra-subduction magmatism is dated between ca. 1400–1040 Ma [*Oliver et al*., 1998; *Johnson and Oliver*, 2004; *Johnson et al., in press*] and appears to have terminated with the onset of magmatism in the Irumide Belt, and also corresponds with the oldest recorded metamorphic ages in other parts of the Southern Irumide Belt dated at 1043 ± 19 [*Cox et al*., 2002] and 1046 ± 3 [*Schenk and Appel*, 2001, 2002]. We suggest that this represents the time of accretion of the island arcs to the Congo Craton margin. The juxtaposition these young, hot magmatic arcs against an old, cold passive margin may have caused part of the continental lithospheric keel to delaminate, allowing the rise of hot asthenospheric material toward the surface, resulting in a dramatic rise in the continental margin geotherms and the pervasive melting of this margin. A similar scenario has been proposed for Arenig-aged tectono-metamorphism in the Dalradian Supergroup of Scotland when the Midland Valley Arc collided/accreted with the Laurentian passive margin [*Oliver*, 2001].

[14] The low-pressure, high-temperature tectono-metamorphic Irumide Orogenic cycle is more compatible with accretion tectonics and thus negates any type of continental collisions along this margin at this time. This would indicate that this margin of the Congo Craton was not involved with Rodinia amalgamation, i.e., the Congo Craton was not part of Rodinia [*Pisarevsky et al.*, 2003; *Johnson and Oliver*, 2004] (Fig. 5). Clearly, in order to better understand global plate reconfigurations, a first-order-goal must be to unravel the tectono-thermal evolution of metamorphic belts, rather than basing these reconstructions on the broad similarity of geochronological datasets.

Figure 5: Rodinia reconstruction after Pisarevsky *et al.* (2003), illustrating tectonic environments of the Congo-Tanzania-Bangweulu and Kalahari Cratons at ca. 1.0 Ga. Abbreviations: Am – Amazonian craton; Au – Australia; Ba – Baltica; C-A-K – Congo-Angola-Kasai craton; I. Belt – Irumide Belt; Ka – Kalahari craton; KB – Kibaran Belt; La – Laurentia; Ma – Mawson craton; N-N – Namaqua-Natal Belt; P – Pampean Terrane; RP – Rio de la Plata; SC – South China craton; T – Tarim; T-B – Tanzania-Bangweulu cratons; WA – West Africa; ZZB – Zambian Zambezi Belt.

References

Agar, R.A. and Ray, A.K., 1983. The geological map of the Petauke area. Geological Survey of Zambia, Lusaka.

Andersen, L.S. and Unrug, R., 1984. Geodynamic evolution of the Bangweulu block, northern Zambia. Precambrian Research, 25: 187-212.

Barr, M.W.C. and Drysdall, A.R., 1972. The geology of the Sasare area; explanation of degree sheet 1131, SW quarter. 30, Geological Survey of Zambia, Lusaka.

Berman, R. G., 1990. Mixing properties of Ca-Mg-Fe-Mn garnets. American Mineralogist, 75: 328-344.

Cordiner, R.J., 2000. The geology of the Kanona area : explanation of degree sheet 1330, NE quarter. 53, Geological Survey Department of Zambia, Lusaka.

Cox, R.A., Rivers, T., Mapani, B., Tembo, D. and De Waele, B., 2002. New U-Pb data for the Irumide belt: LAM-ICP-MS results for Luangwa Terrane. In: G.S.o. Namibia (Editor), 11th IAGOD Quadrennial Symposium and Geocongress, Windhoek, Namibia, pp. 3.

Daly, M.C., 1986. The tectonic and thermal evolution of the Irumide belt, Zambia. PhD Thesis, University of Leeds, Leeds, 326 pp.

Daly, M.C. and Unrug, R., 1982. The Muva Supergroup, northern Zambia. Transactions of the Geological Society of South Africa, 85: 155-165.

De Waele, B. and Fitzsimons, I.C.W., 2004. The age and detrital fingerprint of the Muva Supergroup of Zambia: Molassic deposition to the southwest of the Ubendian belt, Geoscience Africa 2004, Johannesburg, South Africa, pp. 163.

De Waele, B., Fitzsimons, I.C.W. and Nemchin, A., 2004a. Palaeoproterozoic to Mesoproterozoic deposition, magmatism, and metamorphism at the southeastern margin of the Congo craton: the geological history of the Irumide belt., 20th Colloquium of African Geology, Orléans, France, pp. 127.

De Waele, B., Fitzsimons, I.C.W., Wingate, M.T.D., Mapani, B. and Tembo, F., 2004b. A U-Pb SHRIMP geochronological database for the Irumide belt of Zambia: from Palaeoproterozoic sedimentation to late Mesoproterozoic magmatism., 32nd International Geological Congress, Florence, Italy.

De Waele, B. and Mapani, B., 2002. Geology and correlation of the central Irumide belt. Journal of African Earth Sciences, 35(3): 385-397.

De Waele, B., Wingate, M.T.D., Mapani, B. and Fitzsimons, I.C.W., 2003. Untying the Kibaran knot: A reassessment of Mesoproterozoic correlations in southern Africa based on SHRIMP U-Pb data from the Irumide belt. Geology, 31(6): 509-512.

Hanson, R.E., 2003. Proterozoic geochronology and tectonic evolution of southern Africa. *In:* M. Yoshida, B.F. Windley & S. Dasgupta (Eds.), *Proterozoic East Gondwana: Supercontinent Assembly and Breakup*. Geological Society of London Special Publication **206**, London, pp. 427-463.

Hoisch, T. D., 1990. Empirical calibration of six geobarometers for the mineral assemblage quartz + muscovite + biotite + plagioclase + garnet. Contributions to Mineralogy and Petrology, 104: 225-234.

John, T., Schenk, V. and Tembo, F., 1999. The metamorphic evolution and U/Pb dating of monazites of the southern Irumide belt, SE- Zambia. In: B. De Waele, F. Tembo and R.M. Key (Editors), Abstracts Volume IGCP 419/419. Geological Society of Zambia, Lusaka, pp. 7.

Johns, C.C. et al., 1989. The stratigraphic and structural framework of eastern Zambia: Results of a geotraverse. Journal of African Earth Sciences, 9: 123-136.

Johnson, S., Rivers, T. and De Waele, B., in press. A Review of the Mesoproterozoic to early Palaeozoic magmatic and tectonothermal history of south-central Africa: implications for Rodinia and Gondwana. Journal of the Geological Society of London.

Johnson, S.P. and Oliver, G.J.H., 2004. Tectonothermal history of the Karouera Arc, northern Zimbabwe. Precambrian Research, 130: 71-97.

Ludwig, K.R., 2001a. Isoplot/Ex rev. 2.49, Berkely Geochronology Centre, Berkely, California.

Ludwig, K.R., 2001b. Squid 1.02: A User's Manual. 2, Berkeley Geochronology Center, Berkeley.

Mapani, B., 1999. Tectonic and metamorphic evolution of the Serenje and adjoining areas. In: B. De Waele, F. Tembo and R.M. Key (Editors), Abstracts Volume IGCP 418/419. Geological Society of Zambia, Lusaka, pp. 16.

Mapani, B.S.E., 1992. Stratigraphy and correlation of the Serenje and adjoining areas. Zambian Journal of Applied Earth Sciences, 6(1): 1-8.

Mapani, B.S.E. and Moore, T.A., 1995. The geology of the Serenje area, explanation of degree sheet 1330, NW quarter. 51, Geological Survey Department of Zambia, Lusaka.

Nelson, D.R., 1997. Compilation of SHRIMP U-Pb zircon geochronology data, 1996. 1997/2, Geological Survey of Western Australia, Perth, Australia.

Oliver, G.J.H. 2001. Reconstruction of the Grampian episode in Scotland: its place in the Caledonian Orogeny. *Tectonophysics* **332**, 23-49.

Oliver, G.J.H., Johnson, S.P., Williams, I.S. and Herd, D.A., 1998. Relict 1.4 Ga oceanic crust in the Zambezi Valley, northern Zimbabwe: Evidence for Mesoproterozoic supercontinental fragmentation. Geology, 26: 571-573.

Phillips, K.A., 1964. The Geology of the Lusandwa River area; Explanation of Degree Sheet 1331, SE Quarter. 13, Geological Survey of Zambia, Lusaka.

Phillips, K.A., 1965. The Geology of the Petauke - Mwanjawantu area; Explanation of Degree Sheet 1431, NW and part of SW quarters. 15, Geological Survey of Zambia, Lusaka.

Pisarevsky, S.A., Wingate, M.T.D., Powell, C.M., Johnson, S. & Evans, D.A.D., 2003. Models of Rodinia assembly and fragmentation. *In:* M. Yoshida, B. Windley & S. Dasgupta (Eds.), *Proterozoic East Gondwana: Supercontinent Assembly and Breakup*. Geological Society of London Special Publication **206**, 35– 55.

Rainaud, C., Master, S., Armstrong, R.A. and Robb, L.J., 2003. A cryptic Mesoarchean terrane in the basement to the central African Copperbelt. Journal of the Geological Society of London, 160: 11-14.

Ramsay, C.R. and Ridgway, J., 1977. Metamorphic patterns in Zambia and their bearing on problems of Zambian tectonic history. Precambrian Research, 4: 321-337.

Ridgway, J. and Ramsay, C.R., 1986. A provisional metamorphic map of Zambia - explanatory notes. Journal of African Earth Sciences, 5(5): 441-446.

Rubatto, D. and Gebauer, D., 2000. Use of Cathodoluminescence for U-Pb Zircon dating by Ion Microprobe: Some examples from the Western Alps. In: M. Pagel, V. Barbin, P. Blanc and D. Ohnenstetter (Editors), Cathodoluminescence in Geosciences. Springer-Verlag, Berlin, pp. 373-400.

Schenk, V. and Appel, P., 2001. Anti-clockwise P-T path during ultrahigh-temperature (UHT) metamorphism at ca. 1050 Ma in the Irumide Belt of Eastern Zambia. Berichte der Deutschen Mineralogischen Gesellschaft, Beihefte zum European Journal of Mineralogy, 13: 161.

Schenk, V. and Appel, P., 2002. UHT-metamorphism in the Irumide belt of Zambia: an anti-clockwise P-T path and concordant monazite age at 1.05 Ga. In: N. Ennih and G. Abdelsalam Mohamed (Editors), 19th Colloquium of African Geology, El Jadida, Morocco, pp. 165.

Simpson, J.G., 1967. The geology of the Chinyunu area; explanation of degree sheet 1529, N.W. quarter. Printed by the Govt. Printer, Lusaka,, ix, 70 pp.

Stillman, C.J., 1965. The geology of the Musofu river and Mkushi areas; explanation of degree sheet 1329, part of NW quarter and SW quarter. 12, Geological Survey Department of Zambia, Lusaka.

Thieme, J.G., 1970. The geology of the Mansa area; explanation of degree sheet 1128 parts of NW Quarter and NE Quarter. 26, Geological Survey Department of Zambia, Lusaka.

Thieme, J.G., 1971. The geology of the Musonda Falls area: explanation of degree sheet 1028, SE quarter. 32, Geological Survey Department of Zambia, Lusaka.

Vrána, S., 1979. Metamorphic patterns in Zambia and their bearing on problems of Zambian tectonic history : discussion. Precambrian Research, 8: 127-129.